On the performance of the intermediate Hamiltonian Fock-space coupled-cluster method on linear triatomic molecules: The electronic spectra of NpO2+, NpO22+, and PuO 22+

Infante, Ivan; Gomes, André Severo Pereira; Visscher, Lucas

published in
Journal of Chemical Physics
2006

DOI (link to publisher)
10.1063/1.2244564

document version
Publisher's PDF, also known as Version of record

On the performance of the intermediate Hamiltonian Fock-space coupled-cluster method on linear triatomic molecules: The electronic spectra of NpO2+, NpO22+, and PuO22+

Ivan Infante, André Severo Pereira Gomes, and Lucas Visscher

Citation: J. Chem. Phys. **125**, 074301 (2006); doi: 10.1063/1.2244564
View online: http://dx.doi.org/10.1063/1.2244564
View Table of Contents: http://jcp.aip.org/resource/1/JCPSA6/v125/i7
Published by the American Institute of Physics.

On the performance of the intermediate Hamiltonian Fock-space coupled-cluster method on linear triatomic molecules: The electronic spectra of NpO_2^+, NpO_2^{2+}, and PuO_2^{2+}

Ivan Infante, André Severo Pereira Gomes, and Lucas Visscher[a)]
Section Theoretical Chemistry, Faculty of Sciences, Vrije Universiteit Amsterdam, De Boelelaan 1083, 1081 HV Amsterdam, The Netherlands

(Received 23 May 2006; accepted 6 July 2006; published online 16 August 2006)

In this paper we explore the use of the novel relativistic intermediate Hamiltonian Fock-space coupled-cluster method in the calculation of the electronic spectrum for small actinyl ions (NpO_2^+, NpO_2^{2+}, and PuO_2^{2+}). It is established that the method, in combination with uncontracted double-zeta quality basis sets, yields excitation energies in good agreement with experimental values, and better than those obtained previously with other theoretical methods. We propose the reassignment of some of the peaks that were observed experimentally, and confirm other assignments. © *2006 American Institute of Physics*. [DOI: 10.1063/1.2244564]

I. INTRODUCTION

Considerable attention has been paid to actinide chemistry in recent years, due to the need to find new techniques for storage and reprocessing of spent nuclear fuel.[1–3] One of the most important steps of the plutonium uranium extraction (PUREX) process remains the separation of uranium(VI), plutonium(IV), and neptunium(VI) from fission products with aid of the tributylphosphate (TBP) extractant. In this process Pu^{4+} is complexed with two nitrate ions and two TBP ligands, while the other two elements are extracted in the form of the triatomic actinyls UO_2^{2+} and NpO_2^{2+}.[4]

The small size of these actinyls makes calculations feasible, and their energetical and structural parameters are reasonably well characterized.[5,6] Studies regarding the spectroscopic properties of actinyls focused mainly on the uranyl ion, but some studies have also been performed on neptunyl and plutonyl.[7–9] All three actinyl molecules have rather dense spectra due to the low-lying $5f$ and $6d$ orbitals localized on the metal. This characteristic poses a challenge to the currently available theoretical models, as they should describe the manifestation of relativistic effects as well as the multireference character of many of the states that significantly mix under the influence of spin-orbit coupling (SOC).

Among the theoretical methods that have already been used to investigate the spectra of small actinide compounds, single-reference coupled-cluster (CC) theory, both in its nonrelativistic and relativistic formulations, is arguably the most accurate method to calculate dynamic correlation energy. Its applicability is, however, severely limited due to its inability to handle states which have a considerable multireference character.[10] This has up to now left the spin-orbit complete-active-space second-order perturbation theory (SO-CASPT2) or spin-orbit configuration-interaction (SO-CI) methods as the only choices for qualitative or quantitative determination of spectra of neptunyl and plutonyl.

These methods, however, are not without important drawbacks, namely, (a) SO-CI methods are reasonably good for qualitative studies, but have difficulties in attaining quantitative agreement with experiment due to the lack of size extensivity in the electron correlation treatment and to restrictions on the number of configurations that can be included; and (b) SO-CASPT2, at present found to be the most accurate method employed for these systems, due to its ability to handle the use of larger basis sets, has a steep computational scaling with active space size. This limits the flexibility in choosing a suitable reference space and negatively affects the quality of the calculated spectra.

It is therefore of interest to assess new methods which could describe the electronic spectra of small actinyl ions accurately while still possessing a reasonably low scaling behavior. In this paper we explore the use of the intermediate Hamiltonian Fock-space coupled-cluster (IHFSCC) method[11–14] as an alternative to SO-CASPT2 and SO-CI. This method, while well established and routinely applied in high accuracy calculations of atomic transition energies, has scarcely been applied to molecular systems.[15]

The outline of the paper is as follows: in the Methodology section we outline the characteristics of the IHFSCC method and the computational procedure followed; in Results and Discussion, we first present a short analysis of the f^1 configurations, before moving on to our primary interest, the study of the electronic spectrum of the f^2 systems. The computed bond lengths and symmetric stretch frequencies for these gas phase model systems are also discussed, and we conclude by comparing the results of the IHFSCC method to other type of theoretical methods and experiments and discuss the merits and drawbacks of this method.

II. METHODOLOGY

Fock-space coupled-cluster (FSCC) methods[16] have been quite successful in computing the excitation energies of atoms and molecules with very high accuracy.[17] The methods

[a)]Electronic mail: visscher@chem.vu.nl

scale like standard CC calculation [e.g., $O(N^6)$ for CCSD], but produce an effective Hamiltonian that, upon diagonalization, yields the energy of several states at once. In this family of methods, the IHFSCC approach[18] represents a breakthrough, as it greatly reduces the likelihood of intruder states and associated convergence problems in the solution of the CC equations.

The IHFSCC implementation used is that of the molecular four-component code DIRAC,[19,20] in which the T_1 and T_2 excitation operators are included, giving an IHFSCCSD approach that allows for creation of at most two holes and/or electrons outside the reference closed-shell system. While DIRAC can work with various relativistic Hamiltonians, in this application we have used the standard Dirac-Coulomb Hamiltonian, which is capable of describing the strong relativistic and SOC effects in actinyls. As has become common practice in the usage of DIRAC, we neglect contributions from the $(SS|SS)$-type integrals, replacing them by a simple correction,[21] and employ a Gaussian finite nucleus model[22] with this Hamiltonian. As with all FSCC methods, for the IHFSCC approach the reference state must be a single determinant. This means, in the case of PuO_2^{2+} and NpO_2^{+}, that we start, respectively, from the PuO_2^{4+} and NpO_2^{3+} species and add the missing two open-shell electrons in the IHFSCC step. This amounts to the addition of two particles in the P space, following the sequence

$$\left.\begin{matrix}\mathrm{NpO_2^{3+}}\\ \mathrm{PuO_2^{4+}}\end{matrix}\right\}(0h,0p) \rightarrow \left.\begin{matrix}\mathrm{NpO_2^{2+}}\\ \mathrm{PuO_2^{3+}}\end{matrix}\right\}(0h,1p) \rightarrow \left.\begin{matrix}\mathrm{NpO_2^{+}}\\ \mathrm{PuO_2^{2+}}\end{matrix}\right\}(0h,2p), \tag{1}$$

which is equivalent to calculating the first and second electron affinities for these highly charged systems. The restriction to two creation operators means that quintet states, important at higher energies, are not included. Such states belong to the $(1h,3p)$ sector of Fock space not yet available in the currently CCSD-based implementation.

The equilibrium geometries and harmonic frequencies for the ground and some of the excited states were determined by fitting tenth-order polynomials on discrete representations of the potential energy surfaces. As these molecules are known to be linear in their ground state, we have only considered the displacements along the symmetric stretch of the An–O bonds (An=Pu,Np). Under these circumstances, it is possible to exploit linear symmetry ($D_{\infty h}$) with the DIRAC program. Due to limitations in the computational resources, we did not explore displacements along the other vibrational modes, as the lowering of symmetry brought about by displacements along the asymmetric ($C_{\infty v}$) and bending modes (C_{2v}) would have increased the computational costs significantly.

Since the starting point in the self-consistent-field (SCF) calculations were ions with a +2 charge higher than the actual species, it was necessary to ensure that the ordering of the spinors, particularly in the highest occupied molecular orbital-lowest unoccupied molecular orbital (HOMO-LUMO) region, was consistent and adequate for the subsequent correlation treatment. This made us reorder the spinors in some cases, particularly for bond lengths larger than the equilibrium distance, in such a manner that the $5f$ shells in the starting species were always left empty.

The number of electrons correlated, apart from the two electrons that are included during the IHFSCC treatment, is 24; 10 in spinors of g symmetry and 14 electron in spinors of u symmetry. The virtual space was truncated by excluding spinors with energies larger than 6 a.u. This cutoff is consistent with our more extensive work on UO_2 that will be reported separately.[23]

For the IHFSCC calculations, a partitioning of the P,Q spaces, hereby named "IH-u," was employed for all systems considered. In this partitioning 25 spinors of u symmetry were included in the P space. The P space was further partitioned as follows: the six lowest-lying unoccupied $5f$ spinors from the Pu and Np atoms were included in the P_m space, and the remaining $7p$ and $5f^{\sigma}$ spinors placed in the P_i space. In the orthogonal Q space all virtual spinors of g symmetry, and the spinors of u symmetry not included in the $P=P_m+P_i$, were included. To check convergence with active space size, for PuO_2^{2+} and NpO_2^{+} a second partitioning, hereby named "IH-u+g," was also explored. This consisted of the same P_m space as in IH-u, but with 20 spinors of g symmetry added to the P_i space, in order to have a more balanced description of the P space. The calculations with the latter are substantially more demanding and turned out to give negligible differences in excitation energies for states up to 30 000 cm^{-1} relative to the IH-u space.

The basis set employed for the actinides was that of double-zeta quality developed by Dyall.[24] These sets were used in their uncontracted form and are of size $26s23p17d10f1g1h$. For oxygen the valence correlation-consistent triple-zeta (cc-pVTZ) set of Dunning[25] was used, also in uncontracted form. It should be noted that the TZ set was used here instead of the DZ set due to the need to add additional tight functions in a relativistic calculation that uses a nonrelativistic basis set. We also performed exploratory runs using a TZ quality basis set on the actinide element $(33s29p20d12f3g2h)$ on the equilibrium bond distances. As there was little variation upon enlargement (the excited states are shifted at most by about 200 cm^{-1} for each of the excited states) and the computational cost for each point on the potential energy surface scan was greatly increased, we have opted to employ the uncontracted DZ set on the heavy element.

III. RESULTS AND DISCUSSION

A. Electronic structure of the ground state of NpO_2^{3+} and PuO_2^{4+}

As previously noted, to study the electronic spectrum of NpO_2^{+} and PuO_2^{2+} using the IHFSCC approach one has to start from a closed-shell model molecule, and then proceed by computing the first and second electron affinities successively. Before discussing the results for NpO_2^{+} and PuO_2^{2+}, we first analyze the relative ordering of the virtual orbitals of NpO_2^{3+} and PuO_2^{4+}, as these give a first indication of the expected low-lying states of the f^2 ions. The ordering of the $5f$ orbitals is presented in Table I. It should be noted that the

TABLE I. Correlated electron affinities of the $5f$, $7s$, and $6d$ orbitals for the UO_2^{2+}, NpO_2^{3+}, and PuO_2^{4+} molecules computed from sector (0,1) of the IHFSCC calculations. The correlation space was $(24e/6$ a.u.), with a $(17g,20u)$ P model space. All calculations were performed at the equilibrium bond distance of 1.770 Å for UO_2^+, 1.701 Å for NpO_2^{2+}, and 1.645 Å for PuO_2^{3+}. The assignment of the experimental transitions (Ref. 37) in parentheses is uncertain. The excitation energies are given in cm^{-1}.

					Experiment on NpO_2^{2+}		
Spin	UO_2^+	NpO_2^{2+}	PuO_2^{3+}	NpO_2^{2+} SO-CI[a]	H_2O[b]	$Cs_2UO_2Cl_4$[c]	$CsUO_2(NO_3)_3$[d]
$5f^{\phi}_{5/2u}$	0	0	0	0	0	0	0
$5f^{\delta}_{5/2u}$	2 376	3 544	5 746	447	⋯	1000	⋯
$5f^{\phi}_{7/2u}$	5 736	7 227	8 990	5515	6 760	6880	6459
$5f^{\delta}_{5/2u}$	6 843	8 929	11 907	6565	81 80	7990	9420
$6d^{\delta}_{3/2g}$	16 820	42 524	68 400	⋯	⋯	⋯	⋯
$7s^{\sigma}_{1/2g}$	18 479	51 276	84 179	⋯	⋯	⋯	⋯
$6d^{\delta}_{5/2g}$	20 642	47 443	74 493	⋯	⋯	⋯	⋯
$5f^{\pi}_{1/2u}$	20 764	29 441	41 312	⋯	(17 990)	⋯	⋯
$5f^{\pi}_{3/2u}$	24 535	33 856	45 747	⋯	(21 010)	⋯	⋯
$7p^{\pi}_{1/2u}$	59 179	103 844	146 927	⋯	⋯	⋯	⋯
$7p^{\pi}_{3/2u}$	62 170	107 330	152 277	⋯	⋯	⋯	⋯
$5f^{\sigma}_{1/2u}$	69 317	85 553	107 476	⋯	⋯	⋯	⋯
$7p^{\sigma}_{1/2u}$	74 148	119 663	164 003	⋯	⋯	⋯	⋯

[a]Reference 7.
[b]Reference 37.
[c]Reference 34.
[d]Reference 33.

energies, given in relative energies for ease of comparison with experimental results, are obtained not from the energies of the virtual Hartree-Fock orbitals of the closed-shell systems, but rather from the excitation energies, calculated with the IHFSCC method for the f^1 molecules. These energies are thus relative to the $^2\Phi_u$ ground state that results from occupying the $5f^{\phi}_{5/2}$ orbital. For comparison we also show the first electron affinities for the UO_2^{2+} molecule, which is isoelectronic with NpO_2^{3+} and PuO_2^{4+}.

A qualitative model for the electronic structure of actinyl ions has been given by Matsika and co-workers.[7,26] The lowest two unoccupied orbitals are the nonbonding $5f^{\phi}$ and $5f^{\delta}$ orbitals, which are fully localized on the metal ion. The higher unoccupied orbitals are the antibonding combinations of the oxygen $2p$ and metal $5f^{\pi}$ and $5f^{\sigma}$ orbitals that are also mainly localized on the metal. The nonbonding $6d^{\delta}$ orbital lies relatively high in neptunyl and plutonyl and only plays a role in explaining the observed spectral intensities.[26] In Fig. 1 we show the f^1 affinities (in absolute values) computed with the IHFSCC method. The increasing nuclear charge, going from U to Pu, leads to a stronger binding of the electrons in these isoelectronic systems. The lowering of the $5f$ level is the most pronounced and results in bringing the less shifted $6d$ and, in particular, the $7s$ and $7p$ levels, at too high energies to be of relevance in Np(V) and Pu(VI). All low-lying excited states are thus well described in terms of the $5f^2$ configuration only. In UO_2 the situation is different, since for U(IV) the $6d$, $7s$, and $7p$ orbitals all lie at similar energies as the $5f$'s, yielding a denser and more complicated spectrum more easily perturbed by intermolecular interactions. The UO_2 molecule has attracted much attention lately since matrix spectroscopy studies indicate that the ground state in a neon matrix could differ from that in an argon matrix.[23,27–30] An investigation of UO_2 employing the IHFSCC method and including all relevant configurations ($5f^17s^1$, $5f^2$, $5f^16d^1$, and $5f^17p^1$) will be reported separately.[23]

In Table I, the available experimental values for f^1 NpO_2^{2+} are also included. It should be noted that these absorption spectra were measured in water,[31] but studies in other polar solvents and crystals indicate that the transition energies are not much affected by the environment.[32–34] This

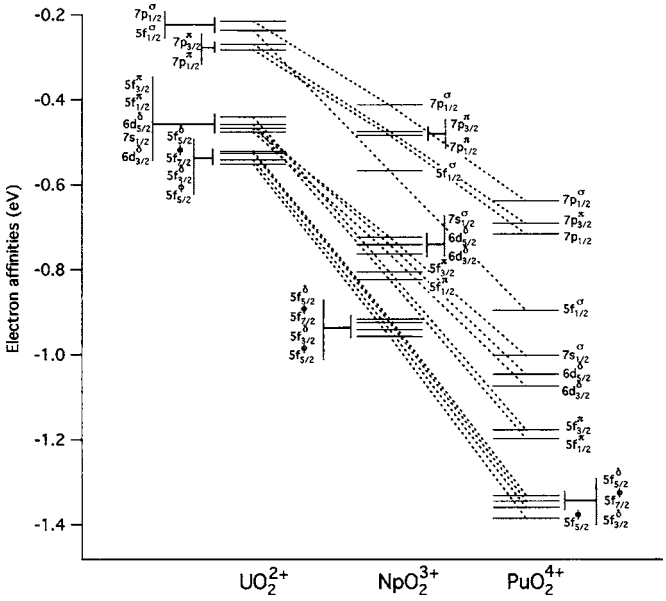

FIG. 1. Orbital energy diagrams including the $5f$, $7s$, $6d$, and $7p$ orbitals for the UO_2^{2+}, NpO_2^{3+}, and PuO_2^{4+} molecules. The correlated values from sector (0,1) of the IHFSCC calculations using the "IH-u" model space are shown. The bond distances are 1.770, 1.701, and 1.645 Å, respectively.

TABLE II. Vertical excitation energies (E, in cm^{-1}) for NpO_2^+, calculated with the IHFSCC method using the "IH-u" model space. The computed energies are evaluated at 1.701 Å (equilibrium bond length). Previous assignment based on SO-CI results from Matsika and Pitzer and the experimental data are also given (Refs. 8 and 37). The assignment of the experimental transitions in parentheses is uncertain.

SO-CI Matsika and Pitzer[a] r_e=1.720 Å		IHFSCC This work r_e=1.701 Å		Expt.[b]		Expt.[c]	
State	E (cm^{-1})	State	E (cm^{-1})	State	E (cm^{-1})	State	E (cm^{-1})
4_g	0	4_g	0	$^3H_4$	0	0	
0_g	3 366	0_g	2 527	Σ_0	⋯	Σ_{0g}	
5_g	4 721	1_g	4 102	Π_1	⋯	Π_{1g}	⋯
1_g	4 938	5_g	5 379	$^3H_5$	6 173	$^3H_{5g}$	⋯
6_g	8 867	0_g	8 628	$^3\Pi_0$	8 953	$^3\Pi_{0g}$	8 953
1_g	9 076	1_g	8 929	$^3\Sigma_1$	9 146	$^3\Sigma_{1g}$	9 116
0_g	9 537	0_g	9 378	$^3\Pi_0$	9 780	$^3\Pi_{0g}$	9 777
0_g	9 708	6_g	9 690	$^3H_6$	⋯	$^3H_{6g}$	⋯
2_g	11 187	2_g	10 056	$^3\Pi_2$	10 208	$^3\Pi_{2g}$	10 202
				vib.	11 160	vib.	10 952
0_g	14 415	0_g	14 105	$^3\Gamma_3$	13 020	$^3\Phi_{2g}$	12 995
4_g	15 249	4_g	14 422	Σ_0	13 824	⋯	⋯
1_g	16 156	1_g	15 031	$^1\Gamma_4$	14 577	$^1\Pi_{1g}$	14 558
0_g	19 647	0_g	16 551	$^3\Sigma_1$	16 220	$^3\Delta_{2g}$	16 221
1_g	21 672	1_g	18 992	$^3\Phi_2$	16 100	⋯	⋯
5_g	22 031	3_g	19 735	Δ_2	16 906	⋯	⋯
1_g	23 079	5_g	19 761	Σ_0	⋯	⋯	⋯
6_g	23 327	6_g	20 035	$^3\Delta_1$	18 116	⋯	⋯
2_g	23 649	2_g	23 1877	Π_1	(19 360)	⋯	⋯
3_g	24 834	2_g	23 322	$^2I_6$	21 008	⋯	21 004
4_g	26 592	4_g	25 119	$^3\Delta_3$	(21 700)	⋯	⋯
⋯	⋯	1_g	25 436	$^3\Pi_0$	22 600	⋯	⋯

[a]Reference 7.
[b]Reference 37.
[c]Reference 8.

suggests that the gas phase excitation energies should be a good approximation for the excited states occurring in solution. From our calculations, the energies of the third and fourth levels are in very good agreement with the excitation energies measured in water. The first excited state lies too low to be seen experimentally. The maximum error for these first two transition energies is 749 cm^{-1}. Comparing these values to those of Matsika and Pitzer,[7] obtained from SO-CI calculations, our results appear to be more accurate, as Matsika and Pitzer's show larger (about 1200–1500 cm^{-1}) discrepancies with respect to the experimental values.

Eisenstein and Pryce[35–37] interpreted the transitions at 17 990 and 21 010 cm^{-1} as belonging to f-f type excitations, occupying the $5f^{\pi}$ orbital. As our computed $5f^{\pi}$ energy is much higher, we believe that these transitions are more likely to be due to charge transfer states in which one of the σ_u electrons in NpO_2^{2+} is excited to a higher level. These transitions were not accessible in our calculations, as the current implementation of the method only considers Fock-space sectors that differ by two creation or annihilation operations from the reference space. Matsika and Pitzer[7] have computed energies of such charge transfer states and found them to lie within this experimental range.

B. Electronic spectrum of NpO_2^{2+} and PuO_2^{2+}

In NpO_2^{2+} and PuO_2^{2+} both open-shell electrons occupy the $5f^{\delta}_{3/2u}$ and the $5f^{\phi}_{5/2u}$ orbitals, resulting in a 4_g ground state. Since all lower excited states also belong to the $5f^2$ configuration, transitions between the ground and these excited states are electric dipole forbidden. The experimental spectra[37,38] are consistent with this picture, since most of the measured peaks have low intensity.[26,36,37,39–42] There is one intense peak at 10 204 cm^{-1} for NpO_2^+ and at 12 037 cm^{-1} for PuO_2^{2+}. The assignment of the spectrum is relatively easier for PuO_2^{2+} than for NpO_2^{2+}, due to the larger splitting of the $5f$ orbitals in the former. Above 20 000 cm^{-1} the assignment becomes less certain for both NpO_2^{2+} and PuO_2^{2+}, as quintet charge transfer states also appear in this region.[7]

In Table II we present all the excitations up to 26 000 cm^{-1} for NpO_2^+ and, in Table III, the excitations up to 34 000 cm^{-1} for PuO_2^{2+}. The experimental spectra were originally interpreted by Eisenstein and Pryce[37] on the basis of semiempirical ligand field calculations. These assignments were later reconsidered on the basis of more accurate calculations.[7,9] However, even in these recent results, there were typical errors of a few thousand wave numbers, making some of the assignments still uncertain. Our new calculations

TABLE III. Vertical excitation energies (E, in cm^{-1}) for PuO_2^{2+}, calculated with IHFSCC method using the "IH-u" model space. The computed energies are evaluated at 1.645 Å (equilibrium bond length). For comparison the results of Maron *et al.* (Ref. 43) and Clavaguera-Sarrio *et al.* (Ref. 9) are shown, along with the experimental data (Reference 38).

SDCI+Q+SO Maron *et al.*[a] r_e=1.699 Å		CASPT2+SO Clavaguera-Sarrio *et al.*[b] r_e=1.677 Å		IHFSCC This work r_e=1.645 Å		Expt.[c]	
State	E (cm^{-1})	State	E (cm^{-1})	State	E (cm^{-1})	State	E (cm^{-1})
4_g	0	4_g	0	4_g	0	$^3H_4$	0
0_g	4 295	0_g	4 190	0_g	2 530	Σ_0	⋯
5_g	6 593	1_g	6 065	1_g	4 870	Π_1	⋯
1_g	7 044	5_g	8 034	5_g	6 700	$^3H_5$	⋯
0_g	7 393	0_g	12 874	0_g	10 334	$^3\Pi_0$	10 185
6_g	7 848	1_g	12 906	1_g	10 983	Σ_1	10 500
0_g	9 4115	6_g	14 326	0_g	11 225	$^3\Pi_0$	10 700
1_g	12 874	0_g	14 606	6_g	11 651	$^3H_6$	⋯
2_g	14 169	2_g	14 910	0_g	12 326	$^3\Pi_2$	12 037
						vib.	12 660
5_g	16 984	⋯	⋯	0_g	16 713	$^1\Gamma_4$	15 420
4_g	23 091	⋯	⋯	1_g	17 737	Σ_0	16 075
1_g	27 005	⋯	⋯	4_g	18 565	Σ_1	17 800
6_g	30 254	⋯	⋯	0_g	20 029	$^3\Gamma_3$	19 100
3_g	33 164	⋯	⋯	1_g	22 703	Σ_0	19 810
0_g	33 314	⋯	⋯	6_g	22 889	$^3\Phi_2$	22 200
4_g	33 318	⋯	⋯	5_g	23 022	$^1H_5$	21 840
3_g	33 366	⋯	⋯	3_g	29 710	Π_1	⋯
2_g	33 388	⋯	⋯	2_g	32 198	Δ_2	⋯
1_g	34 520	⋯	⋯	0_g	32 759	$^3\Gamma_4$	⋯
0_g	35 210	⋯	⋯	1_g	34 080	$^1I_6$	⋯
2_g	35 670	⋯	⋯	4_g	34 702	$^1I_6$	⋯
1_g	36 703	⋯	⋯	2_g	34 982	$^3\Delta_1$	⋯

[a]Reference 43.
[b]Reference 9.
[c]Reference 38.

improve upon the excitation energies computed previously since we include all relativistic effects from the start and could also correlate more electrons, but a shortcoming is that we are not yet able to calculate oscillator strengths with the current IHFSCC implementation. We therefore resorted to estimating the shape and intensities of the expected peaks on the basis of the composition of the excited states, shown in Table IV. Eisenstein and Pryce[36] have previously argued that transitions between states that differ only on the sign of the z component of the angular momentum, L_z, of one of the two unpaired electrons have to be narrow. This occurs because the charge distribution remains basically unchanged when going from the ground to the excited state. For excitations that involve a change of the absolute value of L_z, the peaks are broader due to vibrational excitations. This type of reasoning, combined with the fact transitions to doubly excited states should have a low intensity, gives sufficient information to assign the spectra of NpO_2^+ and PuO_2^{2+} on the basis of our data.

From Table IV one can furthermore see the high degree of similarity of the two isoelectronic actinyl ions. There are in general only slight differences in the values of the contributions from different configurations (for instance, the ground state of PuO_2^{2+} is more mixed than the NpO_2^+ ion, with more contribution of the higher-lying $5f^{\pi}_{3/2u}$ orbital), so the two spectra can be discussed together. To better structure the discussion about the assignments, we have divided the spectra into three regions, each possessing some features that are used for the interpretation of the experiment.

1. Region I: from 0 to 7000 cm^{-1}

These three excited states differ by a single excitation from the ground state. In all cases there is a dominant determinant in which one electron is found in either the $5f^{\delta}_{3/2u}$ or $5f^{\phi}_{5/2u}$ orbital, both of which are occupied in the ground state. This region is not well sampled experimentally and therefore a clear comparison with our calculated data cannot be given. We confirm the original assignment of the peak at 6173 cm^{-1} for the NpO_2^+ ion as a 5_g state[37] with a slightly lower computed energy of 5379 cm^{-1} for this $4_g \rightarrow 5_g$ transition.

2. Region II: from 7000 to 13 000 cm^{-1}

In this region we find an excellent agreement with the experimental transition energies for both the neptunyl and plutonyl ions, with errors of about few hundred wave num-

TABLE IV. Composition (in %) of the ground and some of the lowest excited states for NpO_2^+ and PuO_2^{+2}, together with the spinors occupied in the different IHFSCC sectors with respect to the closed shell species NpO_2^{3+} and PuO_2^{4+}. All values are obtained at the calculated equilibrium geometries (r_e=1.701 and 1.645 Å, respectively) for the "IH-u" model space.

	IHFSCC configuration		Weight (%)	
State	$(0h,2p)$	$(0h,1p)$	NpO_2^{+2}	PuO_2^{+2}
4_g	$5f^{\delta}_{3/2u}$	$5f^{\phi}_{5/2u}$	94	81
	$5f^{\pi}_{3/2u}$	$5f^{\phi}_{5/2u}$	4	16
0_g	$5f^{\phi}_{5/2u}$	$5f^{\phi}_{-5/2u}$	59	70
	$5f^{\delta}_{3/2u}$	$5f^{\delta}_{-3/2u}$	32	18
1_g	$5f^{\delta}_{-3/2u}$	$5f^{\phi}_{5/2u}$	80	71
	$5f^{\phi}_{-5/2u}$	$5f^{\phi}_{7/2u}$	11	12
	$5f^{\delta}_{-3/2u}$	$5f^{\delta}_{5/2u}$	4	13
5_g	$5f^{\phi}_{5/2u}$	$5f^{\delta}_{5/2u}$	55	56
	$5f^{\delta}_{3/2u}$	$5f^{\phi}_{7/2u}$	43	36
0_g	$5f^{\phi}_{5/2u}$	$5f^{\delta}_{-5/2u}$	49	49
	$5f^{\delta}_{5/2u}$	$5f^{\phi}_{-5/2u}$	49	49
1_g	$5f^{\delta}_{-3/2u}$	$5f^{\delta}_{5/2u}$	55	41
	$5f^{\phi}_{-5/2u}$	$5f^{\phi}_{7/2u}$	28	37
	$5f^{\delta}_{-3/2u}$	$5f^{\phi}_{5/2u}$	12	10
0_g	$5f^{\phi}_{5/2u}$	$5f^{\delta}_{-5/2u}$	29	27
	$5f^{\delta}_{5/2u}$	$5f^{\phi}_{-5/2u}$	29	27
	$5f^{\delta}_{3/2u}$	$5f^{\delta}_{-3/2u}$	24	18
	$5f^{\delta}_{5/2u}$	$5f^{\delta}_{-5/2u}$	6	6
6_g	$5f^{\delta}_{5/2u}$	$5f^{\phi}_{7/2u}$	67	57
	$5f^{\phi}_{5/2u}$	$5f^{\phi}_{7/2u}$	33	43
2_g	$5f^{\delta}_{-3/2u}$	$5f^{\phi}_{7/2u}$	93	82
	$5f^{\Pi}_{-3/2u}$	$5f^{\phi}_{7/2u}$	4	16
0_g	$5f^{\delta}_{5/2u}$	$5f^{\delta}_{-5/2u}$	31	20
	$5f^{\phi}_{5/2u}$	$5f^{\phi}_{-5/2u}$	25	23
	$5f^{\delta}_{5/2u}$	$5f^{\delta}_{-5/2u}$	14	16
	$5f^{\delta}_{5/2u}$	$5f^{\phi}_{-5/2u}$	14	16
	$5f^{\delta}_{3/2u}$	$5f^{\delta}_{-3/2u}$	11	15
4_g	$5f^{\phi}_{3/2u}$	$5f^{\delta}_{5/2u}$	83	72
	$5f^{\pi}_{3/2u}$	$5f^{\delta}_{5/2u}$	5	18
1_g	$5f^{\phi}_{5/2u}$	$5f^{\phi}_{-7/2u}$	43	43
	$5f^{\delta}_{5/2u}$	$5f^{\phi}_{-7/2u}$	38	28
	$5f^{\delta}_{3/2u}$	$5f^{\delta}_{-5/2u}$	11	19
0_g	$5f^{\phi}_{7/2u}$	$5f^{\phi}_{-7/2u}$	35	47
	$5f^{\delta}_{5/2u}$	$5f^{\delta}_{-5/2u}$	27	33
	$5f^{\delta}_{3/2u}$	$5f^{\delta}_{-3/2u}$	21	12
1_g	$5f^{\delta}_{5/2u}$	$5f^{\phi}_{-7/2u}$	56	65
	$5f^{\phi}_{5/2u}$	$5f^{\phi}_{-7/2u}$	23	14
	$5f^{\delta}_{3/2u}$	$5f^{\delta}_{-5/2u}$	20	19
3_g	$5f^{\phi}_{5/2u}$	$5f^{\pi}_{1/2u}$	96	97
5_g	$5f^{\delta}_{3/2u}$	$5f^{\delta}_{7/2u}$	55	50
	$5f^{\phi}_{5/2u}$	$5f^{\delta}_{5/2u}$	44	43
6_g	$5f^{\phi}_{5/2u}$	$5f^{\phi}_{7/2u}$	67	56
	$5f^{\delta}_{5/2u}$	$5f^{\phi}_{7/2u}$	33	43
2_g	$5f^{\phi}_{5/2u}$	$5f^{\pi}_{-1/2u}$	91	96
2_g	$5f^{\delta}_{3/2u}$	$5f^{\pi}_{1/2u}$	93	80
	$5f^{\pi}_{3/2u}$	$5f^{\pi}_{1/2u}$	2	19
4_g	$5f^{\phi}_{5/2u}$	$5f^{\pi}_{3/2u}$	58	62
	$5f^{\phi}_{7/2u}$	$5f^{\pi}_{1/2u}$	37	20
1_g	$5f^{\phi}_{5/2u}$	$5f^{\pi}_{-3/2u}$	89	73
	$5f^{\phi}_{5/2u}$	$5f^{\delta}_{-3/2u}$	2	21

bers. The characteristic feature in both spectra is the intense peak that appears 10 204 cm^{-1} for NpO_2^+ and at 12 037 cm^{-1} for PuO_2^{2+}. A mechanism that can explain the intensity of this dipole-forbidden transition is described in detail by Matsika *et al.*,[26] who considered systems with one, three, and five chloride ions in the equatorial plane. Their calculations show that the ligand field from the latter arrangement gives sufficient mixing of the $5f^{\phi}$ and $6d^{\delta}$ to cause an intense $^3H_{4g} \rightarrow {}^3\Pi_{2g}$ transition.

From the decomposition given in Table IV it is clear that this 2_g state for NpO_2^+ is dominated by a single determinant, accounting for 93% of the total wave function. With respect to the ground state configuration, this state corresponds to the excitation of an electron from the $5f^{\phi}_{5/2u}$ to the $5f^{\phi}_{-7/2u}$ orbital. This is also the case for PuO_2^{2+}, for which the weight of the relevant determinant in the 2_g state is slightly smaller (at 83% of the total wave function), corroborating the assignment of Matsika *et al.*.

The 6_g state is found close to the 2_g state, but it is unclear whether transitions to this state have enough intensity to be detected. Eisenstein and Pryce[37] suggested that the peak at 11 160 cm^{-1} is either due to this state or to vibrational progression of the 2_g transition. Our analysis shows a 6_g wave function dominated by two determinants, where one with the highest weight corresponds to a double excitation from the ground state. Combined with the fact that a transition energy below 10 000 cm^{-1} was obtained, we conclude that the assignment of the 11 160 cm^{-1} peak to 6_g is unlikely, and that the interpretation as a vibrational band is probably correct.

Regarding the assignment of the remaining peaks in region II, there are three other excited states, namely, 0_g, 1_g, and 0_g, that could be contributing. They all arise from orbitals that have the same δ and ϕ characters as the ground state, but with different signs of the L_z component (see Tables II and III). All the peaks should be narrow but differ in intensities. The calculations by Matsika *et al.* show that the transition to the 1_g state is more intense than the ones to the 0_g states. This leads to the conclusion that the peaks (at 9146 cm^{-1} for NpO_2^+ and at 10 500 cm^{-1} for PuO_2^{2+}) should be assigned to the 1_g state. While this interpretation had already been put forward with a good deal of certainty in previous works,[26,37] the IHFSCC results serve as a litmus test for this assignment as we can compare the spacing of the computed and observed peaks.

In the experimental spectrum of NpO_2^+ (Fig. 1 of Ref. 26) three narrow peaks are visible to the right (higher wave length) of the strong 2_g transition. The lowest energy transitions are separated by only 163 cm^{-1}, while the higher energy transitions appear as a well resolved shoulder on the 2_g transition at 9780 cm^{-1}. Of the three peaks, the middle one is clearly the most intense. The relative energies of the 0_g, 1_g, and 0_g states are indeed consistent with this spectrum, with the 1_g appearing in the middle separated by 301 cm^{-1} from the lower 0_g state and by 449 cm^{-1} from the higher 0_g state. The deviations from the experimental peak positions are thus maximally 400 cm^{-1}, which should be considered very good agreement for a gas phase model. In the less resolved PuO_2^{2+} spectrum,[37] the 0_g, 1_g, and 0_g states lie practically in the same band, with the 1_g peak at 10 500 cm^{-1}. This peak has one left shoulder, almost completely resolved at 10 185 cm^{-1}, and one right shoulder, hidden in the 1_g at 10 700 cm^{-1}. In our calculations a similar trend is found, with the lower 0_g and 1_g states again separated by a somewhat larger value (649 cm^{-1}) than the spacing that is experimentally observed (315 cm^{-1}). The calculated upper 0_g state is only 240 cm^{-1} higher than the 1_g, which is in very good agreement with the fit of the experimental data (where a distance of about 200 cm^{-1} is given).

3. Region III: above 13 000 cm^{-1}

For the higher excited state agreement with experiment cannot be expected to be as good, as there are larger effects due to the surroundings, and the possible presence of charge transfer states. Looking at the experimental spectra,[37,38] in the region we find for both neptunyl and plutonyl peaks with qualitatively similar shapes, with the most intense transition at about 16 000 cm^{-1} surrounded by satellite shoulders. For NpO_2^+ these shoulders are resolved and narrow, while for PuO_2^{2+} they are quite broad.

In our calculations we find five excited states (0_g, 4_g, 1_g, 0_g, and 1_g,) in this region, mainly made up by determinants containing δ and ϕ electrons in open shells. Based on the arguments put forth at the beginning of this section, this means that the associated peaks should be narrow. The oscillator strengths calculated by Matsika *et al.*[26] indicate that the most intense of these peaks should be the 1_g state. Our calculations place this state at 15 031 cm^{-1} for NpO_2^+ and at 17 737 cm^{-1} for PuO_2^{2+}, whereas the experimental positions are almost the same for both ions (16 220 and 16 075 cm^{-1}, respectively).

Matsika *et al.*, however, suggested that this peak results from a transition to a $^3\Delta_{2g}$ state arising from occupation of the $5f^{\pi}$ orbital. As already discussed in the previous section on NpO_2^{2+}, the $5f^{\pi}$ orbital is at a rather high energy relative to the $5f^{\phi}$ and $5f^{\delta}$. Consequently, all states with significant $5f^{\pi}$ character are found too high in energy (around 20 000 cm^{-1} for NpO_2^+ and 30 000 cm^{-1} for PuO_2^{2+}) to be associated with transitions at 16 000 cm^{-1}. While this may be an artifact of our gas phase model, it could also be that the the observed transition is to the 1_g state, rather than the 2_g state. This is particularly the case for PuO_2^{2+}, where it does not seem probable that the the surrounding water molecules lower this metal-to-metal transition to half the gas phase value. We therefore propose to reassign this transition to the 1_g state.

Another reassignment may be necessary for the experimental peak at 13 020 cm^{-1} for NpO_2^+. This peak was previously assigned to a 3_g state by Eisenstein and Pryce,[37] and later to a 2_g state by Matsika *et al.*[26] In both cases, the composition of this excited state included a $5f^{\pi}$ orbital that we anticipate to get occupied only at much higher energies. It is difficult to assign these peaks with certainty, because the differences in energies involved are rather small. We notice, however, that the calculated 4_g state lies at lower energies than the more intense 1_g for NpO_2^+, while appearing at higher energies for PuO_2^{2+}. This agrees with the experimental spectra, where one small peak at lower energies than the state we assigned as the 1_g is found in the plutonyl spectrum, whereas two peaks are found for neptunyl.

Given the uncertainties related to the position of charge transfer peaks (found slightly above 20 000 cm^{-1} in the calculations of Matsika and Pitzer[7]), we do not attempt to match our computed excitation energies at higher energies with the experimental data.

4. Comparison with previous calculations

Comparing our computed excitation energies for NpO_2^+ with those of Matsika and Pitzer,[7] we see that a more rigorous treatment of electron correlation and relativistic effects indeed results in smaller deviations from experiment. This is so for the lower excited states (below 10 000 cm^{-1}), but also for most of the higher states, especially the important 2_g state, which differs from experiment by less than 200 cm^{-1}, compared to over 1500 cm^{-1} for previous calculations.

More theoretical calculations are available for the plutonyl ion, so the relative accuracy of our results and the strenghts and weaknesses of the IHFSCC method can better be assessed. The calculations of Maron *et al.* [43] and of Clavaguéra-Sarrio *et al.*[9] give rise to a rather similar assignment of the lower excited states, but report excitation energies quite different from ours and from experiment. For instance, the results of Maron *et al.*[43] underestimate the low-lying transitions (region I) and strongly overestimate the upper states (region III), with discrepancies with respect to the experimental transitions of more than 10 000 cm^{-1}. Our calculations show errors on the 1000–2000 cm^{-1} range for these states. The later calculations of Clavaguéra-Sarrio *et al.* are better than those of Maron *et al.*[43] for region II states, but their errors are still quite large (more than 2000 cm^{-1}) when compared to what can be achieved with the IHFSCC method that shows deviations of about 500 cm^{-1}.

C. Potential energy curves

As the IHFSCC method allows the determination of multiple states available in a single calculation, it was quite easy to determine the equilibrium bond distances and vibrational symmetric stretch frequencies for a number of different states. These quantities are shown in Table V. An important difference between these results and those of previous calculations is the difference of the bond lengths for the

TABLE V. Bond lengths (in Å) and harmonic frequencies (in cm^{-1}) for the first 14 states of NpO_2^+ and PuO_2^{2+}, derived from potential energy surfaces for the symmetric stretch. These surfaces were obtained with the IHFSCC method using the "IH-u" model space.

	NpO_2^+		PuO_2^{2+}		
State	r_c (Å)	ω_e (cm^{-1})	State	r_c (Å)	ω_e (cm^{-1})
4_g	1.700	1073	4_g	1.643	1144
0_g	1.701	1061	0_g	1.654	1048
1_g	1.699	1069	1_g	1.643	1162
5_g	1.699	1080	5_g	1.637	1334
0_g	1.699	1081	0_g	1.637	1361
1_g	1.698	1072	1_g	1.637	1351
0_g	1.695	1082	0_g	1.634	1324
6_g	1.701	1075	6_g	1.642	1087
2_g	1.697	1063	2_g	1.636	1281
0_g	1.691	1093	0_g	1.637	1332
4_g	1.698	1086	1_g	1.630	1284
1_g	1.701	1083	4_g	1.636	1400
0_g	1.701	1179	0_g	1.637	1439
1_g	1.724	1564	1_g	1.640	1377

ground state of both molecules. For neptunyl, the bond length is about 0.02 Å shorter than the value given by Matsika and Pitzer,[7] whereas for plutonyl the bond length is about 0.05 Å shorter than that reported by Clavaguéra-Sarrio *et al.*[9] and 0.03 Å shorter than that given by Maron *et al.*.[43] These differences could be due to the inclusion of 6*p* orbitals in the correlated active space in our calculations, allowing the oxo ligands to move closer to the actinide, but we have not investigated this in detail.

The differences in the calculated excited energies shown here and those of previous works decrease to some extent if IHFSCC calculations are performed at the corresponding equilibrium geometries, thus indicating that part of these discrepancies are due to geometrical effects. We observed, however, that also in these situations the IHFSCC calculations generally show a better agreement with experiment.

The harmonic frequencies of the ground state of neptunyl and plutonyl differ by about 69 cm^{-1} (1073 and 1144 cm^{-1}), which is of course mainly due to the difference in charge. It is interesting that the frequencies for the low-lying excited states of neptunyl are very similar to that of the ground state whereas for plutonyl variations of up to 200–300 cm^{-1} are seen. Comparison to experimental data is difficult as it is well known that solvation and complexation lower the vibrational frequencies of actinyls considerably.[44] Madic *et al.*[45] gave Raman data for these ions in aqueous solution. The difference in values for the symmetric stretch of NpO_2^+ and PuO_2^{2+} (767 and 833 cm^{-1}, respectively) of 66 cm^{-1} is remarkably similar to our computed gas phase difference of 71 cm^{-1}.

IV. CONCLUSIONS

In this work we have investigated the ground and excited states of the actinyl ions NpO_2^+ and PuO_2^{2+}. While the spectra of these ions had been studied before, there was still a good deal of uncertainty with respect to the ordering and spacing of different electronic states. In this work we were able to improve upon previous calculations on both aspects. First, we have established with greater certainty that the experimentally most intense peak found for both the actinyl ions has a 2_g symmetry. Second, the average errors we obtain compared to previous calculations are much smaller so that more definite assignments of these spectra could be made. This is particularly important for the higher excited states, where results from previous calculations varied considerably.

The use of the IHFSCC method allowed for the economical determination of several electronic states at once, while accurately describing both static and dynamic correlation energies. The IHFSCC method in its current form, however, is not without drawbacks. What is important is the limitation on the Fock-space sectors that are implemented. For instance, by using only sector $(0h,2p)$ only triplet f^2 states can be described, making charge transfer states of the neptunyl ion unaccessible. For quintet states, a mixed sector $(1h,3p)$ must be employed, but it is yet to be implemented in the DIRAC code. Another drawback is related to issues of convergence, which still demand experimentation with the *P*, *Q* partitioning, and prevent the method to be used in a "black-box" manner that is desired when using the method for larger and more complex systems.

ACKNOWLEDGMENTS

The authors wish to thank the Netherlands Organization for Scientific Research for financial support via the "Jonge Chemici" programme and like to acknowledge stimulating discussions with Dr. Ephraim Eliav and Professor Uzi Kaldor on the application of their IHFSCC methods. This research was performed in part using the Molecular Science Computing Facility (MSCF) in the William R. Wiley Environmental Molecular Sciences Laboratory, a national scientific user facility sponsored by the U.S. Department of Energy's Office of Biological and Environmental Research and located at the Pacific Northwest National Laboratory, operated for the Department of Energy by Battelle.

[1] K. L. Nash, Solvent Extr. Ion Exch. **11**, 729 (1993).
[2] K. L. Nash, R. E. Barrans, R. Chiarizia, M. L. Dietz, M. Jensen, and P. G. Rickert, Solvent Extr. Ion Exch. **18**, 605 (2000).
[3] E. P. Horwitz, D. G. Kalina, H. Diamond, G. F. Vandegrift, and W. W. Schulz, Solvent Extr. Ion Exch. **3**, 75 (1985).
[4] N. C. Rasmussen, *Technologies for Separations and Transmutations* (National Academy, Washington, 1996).
[5] J. P. Bladeau, S. A. Zygmunt, L. A. Curtiss, D. T. Reed, and B. E. Bursten, Chem. Phys. Lett. **310**, 347 (1999).
[6] C. Clavaguera-Sarrio, V. Brenner, S. Hoyau, C. J. Marsden, P. Millie, and J. P. Dognon, J. Phys. Chem. B **107**, 3051 (2003).
[7] S. Matsika and R. M. Pitzer, J. Phys. Chem. A **104**, 4064 (2000).
[8] S. Matsika, Z. Zhang, S. R. Brozell, J. P. Bladeau, and R. M. Pitzer, J. Phys. Chem. A **105**, 3825 (2001).
[9] C. Clavaguera-Sarrio, V. Vallet, D. Maynau, and C. J. Marsden, J. Chem. Phys. **121**, 5312 (2004).
[10] I. Infante and L. Visscher, J. Chem. Phys. **121**, 5783 (2004).
[11] A. Landau, E. Eliav, and U. Kaldor, Chem. Phys. Lett. **313**, 399 (1999).
[12] A. Landau, E. Eliav, Y. Ishikawa, and U. Kaldor, J. Chem. Phys. **113**, 9905 (2000).
[13] A. Landau, E. Eliav, Y. Ishikawa, and U. Kaldor, J. Chem. Phys. **115**, 6862 (2001).
[14] A. Landau, E. Eliav, Y. Ishikawa, and U. Kaldor, J. Chem. Phys. **121**, 6634 (2004).
[15] M. Musial, L. Meissner, S. A. Kucharski, and R. J. Bartlett, J. Chem. Phys. **122**, 224110 (2005).

[16] D. Mukherjee and S. Pal, *Use of Cluster Expansion Methods in the Open-Shell Correlation Problem* (Academic, New York, 1989).
[17] U. Kaldor, E. Eliav, and A. Landau, in *Relativistic Electronic Structure Theory-Part 1: Fundamentals*, edited by P. Schwerdtfeger (Elsevier, Amsterdam, 2002).
[18] J. P. Malrieu, P. Durand, and J. P. Daudey, J. Phys. A **18**, 809 (1985).
[19] L. Visscher, E. Eliav, and U. Kaldor, J. Chem. Phys. **115**, 9720 (2001).
[20] H. J. Aa. Jensen, T. Saue, L. Visscher *et al.*, DIRAC04, Release 4.1, a relativistic *ab initio* electronic structure program, 2004.
[21] L. Visscher, Theor. Chem. Acc. **98**, 68 (1997).
[22] L. Visscher and K. G. Dyall, At. Data Nucl. Data Tables **67**, 207 (1997).
[23] I. Infante, E. Eliav, L. Visscher, and U. Kaldor (unpublished).
[24] K. G. Dyall (unpublished); basis sets are available from the DIRAC website http://dirac.chem.sdu.dk
[25] T. H. Dunning, J. Chem. Phys. **90**, 1007 (1989).
[26] S. Matsika, R. M. Pitzer, and D. T. Reed, J. Phys. Chem. A **104**, 11983 (2000).
[27] L. Gagliardi, M. C. Heaven, J. W. Krogh, and B. O. Roos, J. Am. Chem. Soc. **127**, 86 (2005).
[28] L. Gagliardi, B. O. Roos, P. A. Malmqvist, and J. M. Dyke, J. Phys. Chem. A **105**, 10602 (2001).
[29] M. F. Zhou, L. Andrews, N. Ismail, and C. Marsden, J. Phys. Chem. A **104**, 5495 (2000).
[30] T. Fleig, H. J. A. Jensen, J. Olsen, and L. Visscher, J. Chem. Phys. **124**, 104106 (2006).
[31] D. Cohen and B. Taylor, J. Inorg. Nucl. Chem. **22**, 151 (1962).
[32] H. A. C. McKay, J. S. Nairn, and M. B. Waldron, J. Inorg. Nucl. Chem. **7**, 167 (1958).
[33] R. G. Denning, J. O. Norris, and W. Brown, Mol. Phys. **46**, 325 (1982).
[34] R. G. Denning, J. O. Norris, and W. Brown, Mol. Phys. **46**, 287 (1982).
[35] J. C. Eisenstein and M. H. L. Pryce, Proc. R. Soc. London, Ser. A **229**, 20 (1965).
[36] J. C. Eisenstein and M. H. L. Pryce, J. Res. Natl. Bur. Stand., Sect. A **69**, 217 (1965).
[37] J. C. Eisenstein and M. H. L. Pryce, J. Res. Natl. Bur. Stand., Sect. A **70**, 165 (1966).
[38] *Gmelin Handbooks of Inorganic Chemistry, Transuranium Elements A2*, 8th ed. (Springer-Verlag, New York, 1973).
[39] R. Sjoblom and J. C. Hindman, J. Am. Chem. Soc. **73**, 1744 (1951).
[40] W. C. Waggener, J. Phys. Chem. **62**, 382 (1958).
[41] T. W. Newton and F. B. Baker, J. Phys. Chem. **61**, 934 (1957).
[42] R. H. Bettsand B. G. Harvey, J. Chem. Phys. **16**, 1089 (1948).
[43] L. Maron, T. Leininger, B. Schimmelpfennig, V. Vallet, J. L. Heully, C. Teichteil, O. Gropen, and U. Wahlgren, Chem. Phys. **244**, 195 (1999).
[44] G. S. Groenewold, A. K. Gianotto, K. C. Cossel, M. J. van Stipdonk, D. T. Moore, N. Polfer, J. Oomens, W. de Jong, and L. Visscher, J. Am. Chem. Soc. **128**, 4802 (2006).
[45] C. Madic, G. M. Begun, D. E. Hobart, and R. L. Hahn, Inorg. Chem. **23**, 1914 (1984).